

21 **Abstract**

22 The objective of this study was to investigate the entire spectra (from visible to the thermal
23 infrared; 0.390 μm -14.0 μm) to retrieve leaf water content in a consistent manner. Narrow-band
24 spectral indices (calculated from all possible two band combinations) and a partial least square
25 regression (PLSR) were used to assess the strength of each spectral region. The coefficient of
26 determination (R^2) and root mean square error (RMSE) were used to report the prediction
27 accuracy of spectral indices and PLSR models. In the visible-near infrared and shortwave
28 infrared (VNIR-SWIR), the most accurate spectral index yielded R^2 of 0.89 and RMSE of 7.60%,
29 whereas in the mid infrared (MIR) the highest R^2 was 0.93 and RMSE of 5.97%. Leaf water
30 content was poorly predicted using two-band indices developed from the thermal infrared
31 ($R^2=0.33$). The most accurate PLSR model resulted from MIR reflectance spectra ($R^2=0.96$,
32 RMSE=4.74% and RMSE_{CV}=6.17%) followed by VNIR-SWIR reflectance spectra ($R^2=0.91$,
33 RMSE=6.90% and RMSE_{CV}=7.32%). Using thermal infrared (TIR) spectra, the PLSR model
34 yielded a moderate retrieval accuracy ($R^2=0.67$, RMSE=13.27% and RMSE_{CV}=16.39%). This
35 study demonstrated that the MIR and SWIR domains were the most sensitive spectral region for
36 the retrieval of leaf water content.

37 **Keywords;** Water stress, remote sensing, VNIR-SWIR, MIR, TIR, statistical models

38

39 **1. Introduction**

40 An accurate estimation of leaf water content permits for example monitoring plant physiological
41 status (Datt 1999), predicting drought risk (Bauer et al. 1986), precision agriculture (Peñuelas et
42 al. 1993; Peñuelas et al. 1997) and assessing the risk of forest fire (Chuvieco et al. 2002).
43 Remote sensing is a promising tool for assessing vegetation water status due to its capability of
44 providing continuous spatial observations over large areas compared to point based
45 measurements in the field (Hunt et al. 1987; Hunt and Rock 1989; Sepulcre-Cantó et al. 2006).

46 Retrieving leaf water content using remote sensing data, has been widely investigated in the
47 visible near infrared (VNIR) and shortwave infrared (SWIR) spectra (Thomas et al. 1971;
48 Danson et al. 1992; Aldakheel and Danson 1997; Ceccato et al. 2001; Cheng et al. 2011). Water
49 molecules in leaves strongly absorb electromagnetic energy in the NIR (0.720 – 1.00 μ m) and
50 SWIR (1.40 – 1.90 μ m) (Thomas et al. 1971; Datt 1999). The estimation of leaf water content
51 using NIR is less effective, and the spectral response is less sensitive with changing leaf water
52 content, compared to the SWIR (Datt 1999). Other studies found that leaf water content is
53 strongly correlated with reflectance and derivative spectra at wavebands between 1.40 – 1.90 μ m
54 while wavebands between 1.90 – 25 μ m are relatively less sensitive to the variation in leaf water
55 content (Danson et al. 1992; Ceccato et al. 2001; Ceccato et al. 2002b; Champagne et al. 2003).
56 The wavebands between 1.40 – 1.90 μ m contain water absorption features and are strongly
57 related to leaf water content (Hunt et al. 1987; Bowman 1989).

58

59

60 Very few studies attempted to estimate leaf water content using the MIR and TIR spectra.
61 However, there are strong specific water absorption features located in the MIR (at 2.90, 4.65,
62 and 6.08 μm) which may potentially be a suitable region for quantifying leaf water status
63 (Wieliczka et al. 1989). Using visible to MIR (0.4 – 5.7 μm), Gerber et al. (2011) recently
64 modeled the Directional Hemispherical Reflectance (DHR) and transmittance spectra of fresh
65 and completely dried leaves. Using two different (independent) datasets, they noticed
66 considerable variation with changing leaf water content in the MIR domain (Gerber et al. 2011).
67 More recently, Fabre et al. (2011) studied the effect of leaf water content on spectral reflectance
68 in the MIR to TIR (3.0–15.0 μm). The variation in spectral response of the three plant species
69 used was more pronounced in the MIR compared to the TIR (Fabre et al. 2011). The variation in
70 MIR spectra with varying leaf water content was quantified and resulted in a high correlation
71 with leaf water content. This strong correlation led to the successful estimation of leaf water
72 content from MIR spectra using various spectral transformation techniques (Ullah et al. 2012c;
73 Ullah et al. 2013).

74 The above studies either used VNIR– SWIR or MIR and TIR but they did not sample the same
75 target for the entire range from visible to thermal infrared to guarantee consistency in
76 measurement. In the current study, we report on research where the same leaf samples were
77 measured simultaneously across the visible to thermal infrared. Moreover, the intermediate water
78 levels were acquired by successively dehydrating leaves. The main objective of this study was to
79 assess the strength of the entire spectra (from visible to thermal infrared) for the estimation of
80 leaf water content. The reflectance and first derivative spectra in the visible to thermal infrared
81 domain were assessed using various water stress indices (e.g. by establishing univariate
82 regression) and partial least square regression (PLSR; a type of multivariate regression analysis).

83

84 **2. Material and Methods**

85 **2.1 Leaf sampling and measurements of leaf water content.**

86 Leaves (six samples per species) were collected from various plant species (Table 1) in the
87 vicinity of the ITC building (in Enschede, the Netherlands) during July and August 2011. Before
88 the first spectral measurements, leaves attached to small twigs, were kept moist in cotton to
89 avoid desiccation (Kumar et al. 2010). The leaves were then progressively dehydrated at room
90 temperature and measurements were taken after every four hours. Before the final reading,
91 leaves were oven dried at 60 °C for one and a half hour. The leaves mass were precisely
92 measured using a digital weight balance with 100 µg accuracy.

93 The leaf water content (LWC_f) was calculated using the following formula (Ullah et al. 2013);

$$94 \quad LWC_f = 100(M_w - M_d) / M_w$$

95 where M_w represents the mass of the wet leaf and M_d is the mass of completely dried leaf (dried
96 in oven for 90 minutes at last succession). LWC_f is the leaf water content relative to wet leaf
97 weight.

98 We sampled 402 measurements from eleven different plant species. The number of leaves
99 sampled per species and the dehydration phases are detailed in Table 1.

100 **Insert Table. 1 about here**

101

102 **2.2 Spectral measurements**

103 The spectral measurements were recorded between 0.390 and 14.0 μm . To cover the entire
104 spectral range (visible, NIR, SWIR, MIR and TIR); two different spectrometers were used for
105 the measurements. The ASD FieldSpec® spectro-radiometer (Analytical Spectral Devices:
106 Boulder, CO, USA) covered the VNIR-SWIR range (0.390–2.50 μm), whereas a Bruker
107 VERTEX 70 FTIR (Fourier transform infrared; Bruker Optics GmbH, Ettlingen, Germany)
108 spectrometer was used to acquire Directional Hemispherical Reflectance (DHR) between 2.50 –
109 14.0 μm . During spectral measurements of the leaf samples, the ASD and Bruker spectro-
110 radiometers were used in random order to minimize the influence of different spectral
111 instruments.

112 An ASD spectrometer, coupled with an integrating sphere, was used to measure reflectance
113 spectra between VNIR and SWIR (0.390–2.50 μm ; comprising 2110 spectral bands). The ASD
114 is a portable spectrometer and can acquired spectra with a sampling interval of 1 nm. Two
115 hundred (200) scans were averaged to a single spectrum in order to minimize the effect of noise
116 (signal variance) on the final correlation analysis (see section 2.5). A calibrated reference
117 standard (with approximately 99% reflectance) was used to convert raw radiance to reflectance.

118 A Bruker VERTEX 70 FTIR acquired DHR spectra between 2.5 and 14.0 μm of the adaxial
119 surface of the leaf. The spectrometer was purged of water vapor and carbon dioxide using
120 nitrogen gas. A Mercury Cadmium Telluride (MCT) detector (cooled with liquid N_2) was used to
121 measure leaf spectra with a spectral resolution of 4^{cm} (Hecker et al. 2011; Ullah et al. 2012a;
122 Zaini et al. 2012). Each spectrum was calibrated using a high reflectance (approximately 0.96)
123 gold plate (infragold; Labsphere reflectance technology). Each spectrum was calculated from
124 the average of 1000 scans.

125 **2.3 Preprocessing of spectra and spectral transformation.**

126 The spectra were smoothed using a Savitsky–Golay filter (Savitzky and Golay 1964), with 15
127 sample points and second order polynomials. The smoothed spectra were then used for
128 calculating different indices and first derivatives reflectance (FDR).

129 **2.4 Narrow band indices.**

130 A narrow band simple ratio, simple difference and normalized difference indices (Hunt and Rock
131 1989; Gao 1996; Peñuelas et al. 1997) were calculated for all band combinations using the
132 reflectance spectra. These indices have been reported in the literature for the VNIR–SWIR (Datt
133 1999; Ceccato et al. 2001; Zygielbaum et al. 2009), but are hardly used in the MIR and TIR
134 (Ullah et al. 2013). Different naming conventions are used for the indices in the VNIR-SWIR
135 and MIR and TIR for their interpretation (see details in Table 2).

136 Narrow band vegetation indices have been successfully used to estimate vegetation parameters
137 (Mutanga and Skidmore 2004; Darvishzadeh et al. 2008). The notion of calculating vegetation
138 indices (i.e. simple ratio, normalized difference indices) are based upon the contrast in the
139 reflectance between two spectral bands (Rouse et al. 1974). In vegetation indices, a limited
140 number of wavebands (which contain most of the information) are used from massive
141 hyperspectral wavebands. The purpose of using vegetation indices is to minimize the variability
142 in reflectance caused by various factors such as illumination condition, instrument noise,
143 atmospheric condition and soil background (van Leeuwen and Huete 1996). To determine the
144 best narrow band index, all possible combination of two bands were calculated and a

145 combination that has the highest R^2 with leaf water content was located (Thenkabail et al. 2000;
146 Mutanga and Skidmore 2004).

147 **Insert Table. 2 about here**

148

149 2.5 Statistical analysis

150 2.5.1 Simple Linear regression

151 Simple linear regression was used to quantify the retrieval accuracy of leaf water content using
152 the calculated indices. The data were randomly divided in to calibration and validation subsets.
153 The model was trained with a calibration subset (n= 268; two third of the entire dataset) and was
154 then used to predict the leaf water content in validation subsets (n= 134; one third of the entire
155 dataset). The predicted leaf water content was plotted against the measured leaf water content,
156 and the accuracy of each index reported using R^2 and RMSE.

157 2.5.2 Partial least square regression (PLSR)

158 A challenge associated with hyperspectral data is a high spectral dimensionality and a high
159 degree of collinearity of the adjacent bands (Vaiphasa et al. 2005). Multivariate regression
160 models based on hyperspectral data suffers from multi-collinearity especially when the numbers
161 of predictors are equal or higher in number than sample observations and the input data lead to a
162 high R^2 (Curran 1989). PLSR is a robust technique which can handle high dimensional
163 hyperspectral datasets for predicting leaf bio-chemicals, while minimizing multi-collinearity and
164 model over-fitting (Thomas and Haaland 1990). This technique has been successfully used to
165 estimate several leaf bio-chemicals (Huang et al. 2004; Asner and Martin 2008; Ramoelo et al.

166 2011). The Partial least square regressions (PLSR) were used to estimate leaf water content from
167 both the reflectance and FDR spectra in the VNIR-SWIR, MIR and TIR. The increased use of
168 PLSR in remote sensing (Lin et al. 2007; Asner and Martin 2008; Darvishzadeh et al. 2008;
169 Ramoelo et al. 2011) is due to the fact that PLSR can process multi-collinear predictors
170 (hyperspectral data) by inputting all spectral bands simultaneously and select uncorrelated
171 variables from a matrix of explanatory variables (Geladi and Kowalski 1986). The PLSR
172 analysis was implemented using the TOMCAT toolbox in MATLAB. The independent variables
173 were first mean centered prior to input to the PLSR. The lowest $RMSE_{CV}$ (RMSE-leave-one-out
174 cross validation) was adopted as criterion to select the optimal number of components for model
175 development (Darvishzadeh et al. 2008). The accuracy of the models using different spectral
176 domains was assessed using R^2 , RMSE and $RMSE_{CV}$.

177 **3. Results**

178 **3.1 Effect of leaf water content on spectral responses**

179 The leaf water content was variably correlated with reflectance across spectral bands (Fig.1). The
180 correlation was low between leaf water and the blue part of the spectrum (0.390–0.430 μm) and
181 increased in the green and red part of the visible spectrum (0.50-0.65 μm ; Fig.1 a). The
182 correlation attained a maximum between 1.4 and 2.2 μm (in the SWIR). In the MIR domain, leaf
183 water content was strongly correlated with the Directional Hemispherical Reflectance (DHR)
184 between 2.50 and 2.70 μm , and the correlation became weaker at 2.7 to 3.6 μm . After 3.6 μm
185 the correlation increased to a maximum between 4.0–5.6 μm (Fig 1 b). In the thermal infrared
186 the correlation plot (Fig.1c) exhibited a flat line.

187

188 **Insert Figure. 1 about here**

189
190
191

3.2 Leaf water content and spectral indices

192 Using visible near infrared and shortwave infrared (VNIR-SWIR) spectra, the narrow-band
193 indices (NDWI, SRWI and DWI) were calculated and leaf water content was estimated based on
194 these indices. The indices with the most sensitive waveband combinations yielded a high R^2
195 (Fig.2) using the calibration dataset. The models derived from the calibration data were applied
196 to the validation datasets in order to predict leaf water content. For the VNIR-SWIR domain, the
197 prediction of leaf water content was high ($R^2=0.86$ (minimum), $RMSE=8.86\%$ (maximum))
198 using the validation datasets. For all possible waveband combinations of the three indices, the
199 most sensitive waveband combinations (with highest R^2) were located in the SWIR region (i.e.
200 the blue rectangle in Fig.2). For the VNIR and SWIR, the NDWI provided more accurate
201 predictions of leaf water content compared to SRWI and DWI (Fig. 3), though it is noted that in
202 all three models (NDWI, SRWI and DWI) the predicted values underestimate the measured leaf
203 water content above approximately 50% leaf water content.

204 **Insert Figure. 2 about here**

205

206 **Insert Figure. 3 about here**

207

208 For the MIR, leaf water content was accurately estimated using narrow-band indices (MNDWI,
209 MSRWI and MDWI). Using the calibration datasets, these indices yielded a high R^2 (Fig. 4).
210 When the calibration model was applied to the independent validation datasets, leaf water

211 content was accurately predicted (i.e. high R^2 and low RMSE) (Fig.5 and Table 3). The indices
212 developed from TIR spectra were less effective in estimating leaf water content. Using TIR, the
213 maximum R^2 achieved was 0.33 (from TNDWI) and lead to a poor estimation (i.e. high RMSE)
214 of leaf water content (Fig.6, Table 3).

215 **Insert Figure. 4 about here**

216

217 **Insert Figure. 5 about here**

218

219 **Insert Table. 3 about here**

220

221 **Insert Figure. 6 about here**

222

223 **3.3 Partial least square regression (PLSR) and leaf water content**

224

225 Using the VNIR-SWIR reflectance spectra, the PLSR models (Fig.7) were slightly more accurate
226 ($R^2=0.91$, RMSE =6.90 % and $RMSE_{CV} =7.32$ %) than the PLSR models developed using the
227 first derivative spectra ($R^2=0.90$, RMSE =7.14% and $RMSE_{CV} = 8.50\%$). The number of
228 wavelength latent factors were equal (8 factors) for both the reflectance and first derivative
229 spectra (Table 4).

230 Using reflectance and first derivative spectra in the MIR, both PLSR models yielded an accurate
231 estimate of leaf water content (Fig.8). The models based on MIR reflectance spectra were more
232 accurate ($R^2 =0.96$, RMSE= 4.74 and $RMSE_{CV}= 6.14$) compared to the model developed from
233 first derivative spectra using MIR ($R^2 =0.93$, RMSE= 5.98 and $RMSE_{CV}= 8.40$). The number of
234 factors involved in the models is detailed in Table 4. The PLSR models based on MIR was more

235 accurate (i.e. high R^2 and low RMSE) than the models developed using VNIR –SWIR spectra.
236 The PLSR regression using TIR spectra, yielded the lowest R^2 (0.67) and highest RMSE
237 (13.27 %) and $RMSE_{CV}$ (16.39) (Fig. 9).

238
239 The PLSR models in all spectral domains (i.e. VNIR-SWIR, MIR and TIR) improved the
240 prediction of leaf water content (i.e. results in a higher R^2 and low RMSE) compared to the
241 narrow band indices. The most significant improvement was noticed for retrieving leaf water
242 content using the TIR reflectance, where R^2 increased from 0.32 to 0.67 and RMSE decreased
243 from 31.83% to 16.39 % (Table 3 and Table 4).

244

245 **Insert Table. 4 about here**

246

247 **Insert Figure. 7 about here**

248

249 **Insert Figure. 8 about here**

250

251 **Insert Figure. 9 about here**

252

253 **4. Discussion**

254 Remote sensing is potentially a viable tool to assess and monitor vegetation parameters from
255 local (point sample) to global scales (Skidmore 2002). In the past, estimation of vegetation water
256 content focused on the VNIR-SWIR (0.3-2.5 μ m). The advent of sensor technology in the MIR
257 (2.5-6.0 μ m) and TIR (8.0-14.0 μ m) enables the assessment and monitoring of vegetation
258 functions or physiological status (Ribeiro da Luz 2006; Ribeiro da Luz and Crowley 2007, 2010;

259 Ullah et al. 2012b). In this study, an empirical relationship between leaf spectra and leaf water
260 content demonstrated that MIR and SWIR were the most sensitive spectral regions ($R^2 \geq 0.86$)
261 for the estimation leaf water content. The TIR showed moderate affinity with leaf water content
262 (maximum $R^2 = 0.67$), however the performance of TIR were less accurate compared to MIR
263 and SWIR.

264 The correlation between reflectance spectra (across visible to thermal infrared) and the leaf water
265 content (Fig. 1) underlined that leaf water content is related to the spectral response, but the
266 strength of the relationship varies across VNIR-SWIR/ MIR and TIR. The spectral response was
267 strongly correlated with leaf water content (Fig.1) in the SWIR (1.4-2.5 μm) and MIR (2.5-2.7
268 μm and 3.7-5.6 μm). The findings of this study are in line with that of the previous studies where
269 two band indices were used for the retrieval of leaf water or biochemical parameters (Hunt and
270 Rock 1989; Gao 1996; Datt 1999; Ceccato et al. 2001; Ceccato et al. 2002a; Ceccato et al. 2002b;
271 Zhang et al. 2012). Using narrow-band indices, the most sensitive waveband combinations were
272 located at 1.60 μm , 1.397 μm (i.e. SWIR) and at 2.65 μm , 3.89 μm and 5.20 μm (i.e. MIR).
273 These selected sensitive wavebands (from narrow-band indices) correspond to the slope and
274 depth of water absorption features in the reflectance spectra (Datt 1999; Ceccato et al. 2001;
275 Cheng et al. 2010; Gerber et al. 2011; Ullah et al. 2012c). The selected wavebands in the SWIR
276 (1.397 μm and 1.60 μm) are related to the absorption features associated with moisture, cellulose
277 and starch in plant leaves (Curran 1989; Thenkabail et al. 2004). The selected wavebands at 3.89
278 μm and 5.20 μm (MIR) are associated with cellulose maxima at 4.0 and 5.2 μm (Fabre et al.
279 2011).

280 The PLSR model of the MIR reflectance spectra yielded the highest accuracy ($R^2= 0.96$, RMSE=
281 4.74% and $RMSE_{CV}= 6.14\%$) (Fig.8) compared to the VNIR-SWIR (Fig.7) and TIR (Fig. 9). The
282 PLSR models derived using first derivative spectra were less accurate than the model developed
283 from reflectance spectra. The lower performance of the first derivative PLSR model may be due
284 to consistent illumination conditions used in the experiment, as well as no influence of
285 background soil/litter reflectance (Elvidge and Chen 1995).

286 The PLSR model is emerging as an alternative to univariate statistical analysis for estimating leaf
287 water content as it selects the most important variables for a parsimonious model (Lin et al. 2007;
288 Asner and Martin 2008; Darvishzadeh et al. 2008; Ramoelo et al. 2011) and can therefore be
289 considered in general to be more practical for such analyses. Compared to narrow band indices,
290 all the PLSR models in their respective spectral domains achieved relatively higher accuracy
291 (Table 3 and Table 4). In this study, using the reflectance and first derivative spectra, the number
292 of PLSR latent factors varied from 4 to 10 (Table 4).

293 The novelty of this study is the simultaneous and consistent sampling of the same target leaf
294 while measuring the whole spectrum (from the visible to thermal infrared) for the retrieval of
295 leaf water content. Integrating various imaging spectrometers data to cover the entire spectral
296 range (i.e. visible to thermal) helps to identify the spectral bands for accurate retrieval of leaf
297 water content at the field level and may provide a foundation for up-scaling to canopy level.

298 **5. Conclusion**

299 This study has used univariate and multivariate statistical techniques to examine the strength the
300 VNIR-SWIR, MIR and TIR for the retrieval of leaf water content. Narrow band indices and
301 PLSR were used in to analyze the spectral data. The strength of each model was assessed by

302 comparing the differences in the R^2 and RMSE and $RMSE_{cv}$. It is concluded that the PLSR
303 models were more accurate (yielded high R^2 and low RMSE) compared to narrow band indices
304 in all spectral domains and is a practical and robust technique compared to univariate statistical
305 analysis for estimating leaf water content. The strength of predicting leaf water content using
306 SWIR and MIR (yielded high R^2 and low RMSE) are higher than TIR. The SWIR and MIR
307 proved highly sensitive spectral regions and hold promise for the estimation of leaf water content.

308 **Acknowledgements**

309 The authors wish to thank the Higher Education Commission (HEC) of Pakistan for funding this
310 PhD research and ITC for the purchase of equipment. The authors acknowledge the help of
311 ITC's GeoScience Laboratory team for their assistance.

312 **References**

- 313 Aldakheel, Y.Y., & Danson, F.M. (1997). Spectral reflectance of dehydrating leaves:
314 measurements and modelling. *International Journal of Remote Sensing*, 18, 3683-3690
- 315 Asner, G.P., & Martin, R.E. (2008). Spectral and chemical analysis of tropical forests: Scaling
316 from leaf to canopy levels. *Remote Sensing of Environment*, 112, 3958-3970
- 317 Bauer, M.E., Daughtry, C.S.T., Biehl, L.L., Kanemasu, E.T., & Hall, F.G. (1986). Field
318 spectroscopy of agricultural crops. *IEEE Transactions on Geoscience and Remote Sensing*, 24,
319 65-75
- 320 Bowman, W.D. (1989). The relationship between leaf water status, gas exchange, and spectral
321 reflectance in cotton leaves. *Remote Sensing of Environment*, 30, 249-255
- 322 Ceccato, P., Flasse, S., & Grégoire, J.-M. (2002a). Designing a spectral index to estimate
323 vegetation water content from remote sensing data: Part 2. Validation and applications. *Remote*
324 *Sensing of Environment*, 82, 198-207
- 325 Ceccato, P., Flasse, S., Tarantola, S., Jacquemoud, S., & Grégoire, J.-M. (2001). Detecting
326 vegetation leaf water content using reflectance in the optical domain. *Remote Sensing of*
327 *Environment*, 77, 22-33

- 328 Ceccato, P., Gobron, N., Flasse, S., Pinty, B., & Tarantola, S. (2002b). Designing a spectral
329 index to estimate vegetation water content from remote sensing data: Part 1 - Theoretical
330 approach. *Remote Sensing of Environment*, 82, 188-197
- 331 Champagne, C.M., Staenz, K., Bannari, A., McNairn, H., & Deguise, J.-C. (2003). Validation of
332 a hyperspectral curve-fitting model for the estimation of plant water content of agricultural
333 canopies. *Remote Sensing of Environment*, 87, 148-160
- 334 Cheng, T., Rivard, B., & Sánchez-Azofeifa, G.A. (2011). Spectroscopic determination of leaf
335 water content using continuous wavelet analysis. *Remote Sensing of Environment*, 115, 659-670
- 336 Cheng, T., Rivard, B., Sánchez-Azofeifa, G.A., Feng, J., & Calvo-Polanco, M. (2010).
337 Continuous wavelet analysis for the detection of green attack damage due to mountain pine
338 beetle infestation. *Remote Sensing of Environment*, 114, 899-910
- 339 Chuvieco, E., Riano, D., Aguado, I., & Cocero, D. (2002). Estimation of fuel moisture content
340 from multitemporal analysis of Landsat Thematic Mapper reflectance data: applications in fire
341 danger assessment. *International Journal of Remote Sensing*, 23, 2145-2162
- 342 Curran, P.J. (1989). Remote sensing of foliar chemistry. *Remote Sensing of Environment*, 30,
343 271-278
- 344 Danson, F.M., Steven, M.D., Malthus, T.J., & Clark, J.A. (1992). High-spectral resolution data
345 for determining leaf water-content. *International Journal of Remote Sensing*, 13, 461-470
- 346 Darvishzadeh, R., Skidmore, A.K., Schlerf, M., Atzberger, C.G., & Cho, M.A. (2008). LAI and
347 chlorophyll estimation for a heterogeneous grassland using hyperspectral measurements. *ISPRS*
348 *Journal of Photogrammetry and Remote Sensing*, 63
- 349 Datt, B. (1999). Remote sensing of water content in Eucalyptus leaves. *Australian Journal of*
350 *Botany*, 47, 909-923
- 351 Elvidge, C.D., & Chen, Z.K. (1995). Comparison of broad-band and narrow-band red and near-
352 infrared vegetation indexes. *Remote Sensing of Environment*, 54, 38-48
- 353 Fabre, S., Lesaignoux, A., Oliosio, A., & Briottet, X. (2011). Influence of water content on
354 spectral reflectance of leaves in the 3-15 μm domain. *IEEE Geoscience and Remote Sensing*
355 *Letters*, 8, 143-147
- 356 Gao, B.C. (1996). NDWI - A normalized difference water index for remote sensing of vegetation
357 liquid water from space. *Remote Sensing of Environment*, 58, 257-266
- 358 Geladi, P., & Kowalski, B.R. (1986). Partial least-squares regression: a tutorial. *Analytica*
359 *Chimica Acta*, 185, 1-17

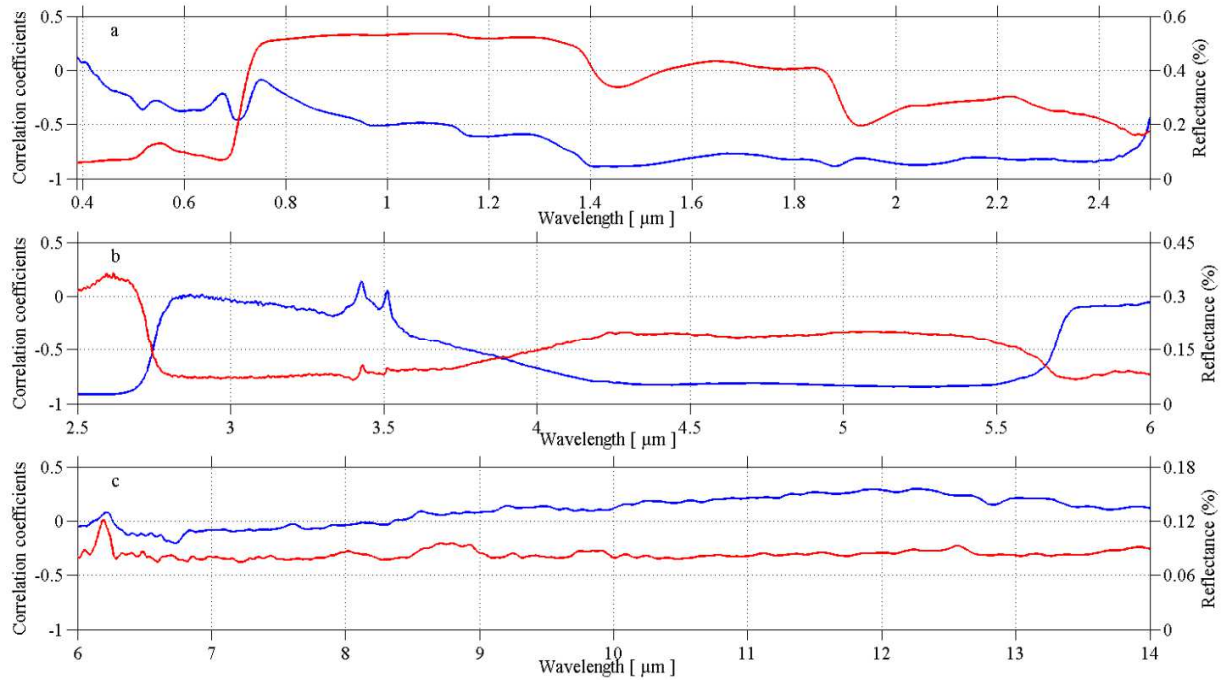
- 360 Gerber, F., Marion, R., Olioso, A., Jacquemoud, S., da Luz, B.R., & Fabre, S. (2011). Modeling
361 directional-hemispherical reflectance and transmittance of fresh and dry leaves from 0.4 μm to
362 5.7 μm with the PROSPECT-VISIR model. *Remote Sensing of Environment*, 115, 404-414
- 363 Hecker, C., Hook, S., Meijde, M.v.d., Bakker, W., Werff, H.v.d., Wilbrink, H., Ruitenbeek, F.v.,
364 Smeth, B.d., & Meer, F.v.d. (2011). Thermal infrared spectrometer for earth science remote
365 sensing applications: instrument modifications and measurement procedures. *Sensors*, 11, 10981-
366 10999
- 367 Huang, Z., Turner, B.J., Dury, S.J., Wallis, I.R., & Foley, W.J. (2004). Estimating foliage
368 nitrogen concentration from HYMAP data using continuum removal analysis. *Remote Sensing of*
369 *Environment*, 93, 18-29
- 370 Hunt, E.R., & Rock, B.N. (1989). Detection of changes in leaf water-content using near-infrared
371 and middle-infrared reflectances. *Remote Sensing of Environment*, 30, 43-54
- 372 Hunt, E.R., Rock, B.N., & Nobel, P.S. (1987). Measurement of leaf relative water-content by
373 infrared reflectance. *Remote Sensing of Environment*, 22, 429-435
- 374 Kumar, L., Skidmore, A.K., & Mutanga, O. (2010). Leaf level experiments to discriminate
375 between eucalyptus species using high spectral resolution reflectance data: use of derivatives,
376 ratios and vegetation indices. *Geocarto International*, 25, 327-344
- 377 Lin, L., Ustin, S.L., & Riano, D. (2007). Retrieval of fresh leaf fuel moisture content using
378 genetic algorithm partial least squares (GA-PLS) modeling. *Geoscience and Remote Sensing*
379 *Letters, IEEE*, 4, 216-220
- 380 Mutanga, O., & Skidmore, A.K. (2004). Narrow band vegetation indices overcome the saturation
381 problem in biomass estimation. *International Journal of Remote Sensing*, 25, 3999-4014
- 382 Peñuelas, J., Gamon, J.A., Griffin, K.L., & Field, C.B. (1993). Assessing community type, plant
383 biomass, pigment composition, and photosynthetic efficiency of aquatic vegetation from spectral
384 reflectance. *Remote Sensing of Environment*, 46, 110-118
- 385 Peñuelas, J., Pinol, J., Ogaya, R., & Filella, I. (1997). Estimation of plant water concentration by
386 the reflectance water index WI (R900/R970). *International Journal of Remote Sensing*, 18, 2869-
387 2875
- 388 Ramoelo, A., Skidmore, A.K., Schlerf, M., Mathieu, R., & Heitkönig, I.M.A. (2011). Water-
389 removed spectra increase the retrieval accuracy when estimating savanna grass nitrogen and
390 phosphorus concentrations. *ISPRS Journal of Photogrammetry and Remote Sensing*, 66, 408-417
- 391 Ribeiro da Luz, B. (2006). Attenuated total reflectance spectroscopy of plant leaves: a tool for
392 ecological and botanical studies. *New Phytologist*, 172, 305-318

- 393 Ribeiro da Luz, B., & Crowley, J.K. (2007). Spectral reflectance and emissivity features of broad
394 leaf plants: prospects for remote sensing in the thermal infrared (8.0-14.0 μm). *Remote*
395 *Sensing of Environment*, 109, 393-405
- 396 Ribeiro da Luz, B., & Crowley, J.K. (2010). Identification of plant species by using high spatial
397 and spectral resolution thermal infrared (8.0-13.5 μm) imagery. *Remote Sensing of*
398 *Environment*, 114, 404-413
- 399 Rouse, J.W., Hass, R.H., & Schell, J.A. (1974). Monitoring the vernal advancement of
400 retrogradation of natural vegetation. In (pp. 1-371). MD, USA: NASA / GSFC
- 401 Savitzky, A., & Golay, M.J.E. (1964). Smoothing and differentiation of data by simplified Least
402 squares procedures. *Analytical Chemistry*, 36, 1627-1639
- 403 Sepulcre-Cantó, G., Zarco-Tejada, P.J., Jiménez-Muñoz, J.C., Sobrino, J.A., Miguel, E.d., &
404 Villalobos, F.J. (2006). Detection of water stress in an olive orchard with thermal remote sensing
405 imagery. *Agricultural and Forest Meteorology*, 136, 31-44
- 406 Skidmore, A.K. (2002). Taxonomy of environmental models in the spatial sciences. In:
407 *Environmental modelling with GIS and remote sensing / A. Skidmore (ed.). London etc. : Taylor*
408 *& Francis, 2002. ISBN 0-415-24170-7 pp. 8-24*
- 409 Thenkabail, P.S., Enclona, E.A., Ashton, M.S., Legg, C., & De Dieu, M.J. (2004). Hyperion,
410 IKONOS, ALI, and ETM+ sensors in the study of African rainforests. *Remote Sensing of*
411 *Environment*, 90, 23-43
- 412 Thenkabail, P.S., Smith, R.B., & De Pauw, E. (2000). Hyperspectral Vegetation Indices and
413 Their Relationships with Agricultural Crop Characteristics. *Remote Sensing of Environment*, 71,
414 158-182
- 415 Thomas, E.V., & Haaland, D.M. (1990). Comparison of multivariate calibration methods for
416 quantitative spectral-analysis. *Analytical Chemistry*, 62, 1091-1099
- 417 Thomas, J.R., Namken, L.N., Oerther, G.F., & Brown, R.G. (1971). Estimating Leaf Water
418 Content by Reflectance Measurements. *Agron. J.*, 63, 845-847
- 419 Ullah, S., Groen, T.A., Schlerf, M., Skidmore, A.K., Nieuwenhuis, W., & Vaiphasa, C. (2012a).
420 Using a Genetic Algorithm as an Optimal Band Selector in the Mid and Thermal Infrared (2.5–
421 14 μm) to Discriminate Vegetation Species. *Sensors*, 12, 8755-8769
- 422 Ullah, S., Schlerf, M., Skidmore, A.K., & Hecker, C. (2012b). Identifying plant species using
423 mid-wave infrared (2.5–6 μm) and thermal infrared (8–14 μm) emissivity spectra. *Remote Sensing*
424 *of Environment*, 118, 95-102

- 425 Ullah, S., Skidmore, A.K., Groen, T.A., & Schlerf, M. (2013). Evaluation of three proposed
426 indices for the retrieval of leaf water content from the mid-wave infrared (2–6 μm) spectra.
427 *Agricultural and Forest Meteorology*, 171–172, 65-71
- 428 Ullah, S., Skidmore, A.K., Naeem, M., & Schlerf, M. (2012c). An accurate retrieval of leaf water
429 content from mid to thermal infrared spectra using continuous wavelet analysis. *Science of The*
430 *Total Environment*, 437, 145-152
- 431 Vaiphasa, C., Ongsomwang, S., Vaiphasa, T., & Skidmore, A.K. (2005). Tropical mangrove
432 species discrimination using hyperspectral data: A laboratory study. *Estuarine Coastal and Shelf*
433 *Science*, 65, 371-379
- 434 van Leeuwen, W.J.D., & Huete, A.R. (1996). Effects of standing litter on the biophysical
435 interpretation of plant canopies with spectral indices. *Remote Sensing of Environment*, 55, 123-
436 138
- 437 Wieliczka, D.M., Weng, S., & Querry, M.R. (1989). Wedge shaped cell for highly absorbent
438 liquids: infrared optical constants of water. *Appl. Opt.*, 28, 1714-1719
- 439 Zaini, N., van der Meer, F., & van der Werff, H. (2012). Effect of Grain Size and Mineral
440 Mixing on Carbonate Absorption Features in the SWIR and TIR Wavelength Regions. *Remote*
441 *Sensing*, 4, 987-1003
- 442 Zhang, L., Zhou, Z., Zhang, G., Meng, Y., Chen, B., & Wang, Y. (2012). Monitoring the leaf
443 water content and specific leaf weight of cotton (*Gossypium hirsutum* L.) in saline soil using leaf
444 spectral reflectance. *European Journal of Agronomy*, 41, 103-117
- 445 Zygielbaum, A.I., Gitelson, A.A., Arkebauer, T.J., & Rundquist, D.C. (2009). Non-destructive
446 detection of water stress and estimation of relative water content in maize. *Geophysical Research*
447 *Letters*, 36
- 448

449 **List of figures**

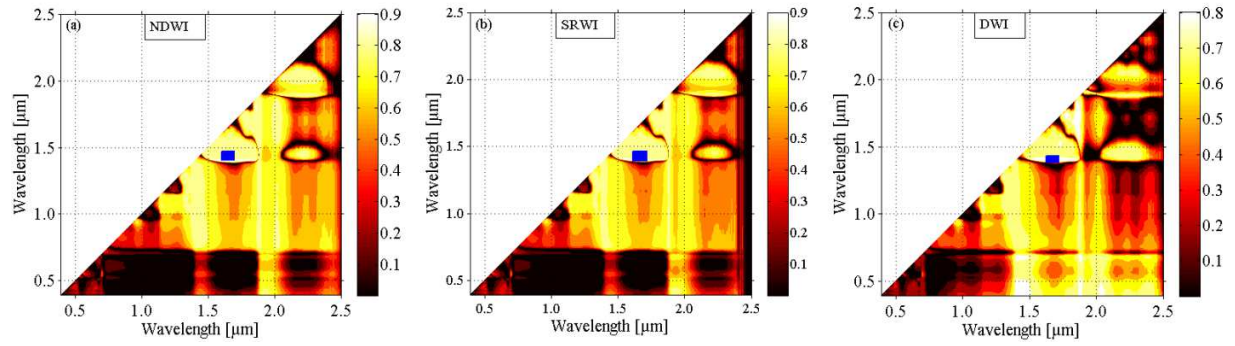
450



451

452 Figure 1. The relationship between spectral reflectance and the leaf water contents in the VNIR-
453 SWIR (a), MIR (b) and TIR (c). The red line represents the average reflectance spectrum while
454 the blue line is the correlation coefficient between leaf water content and spectral response.

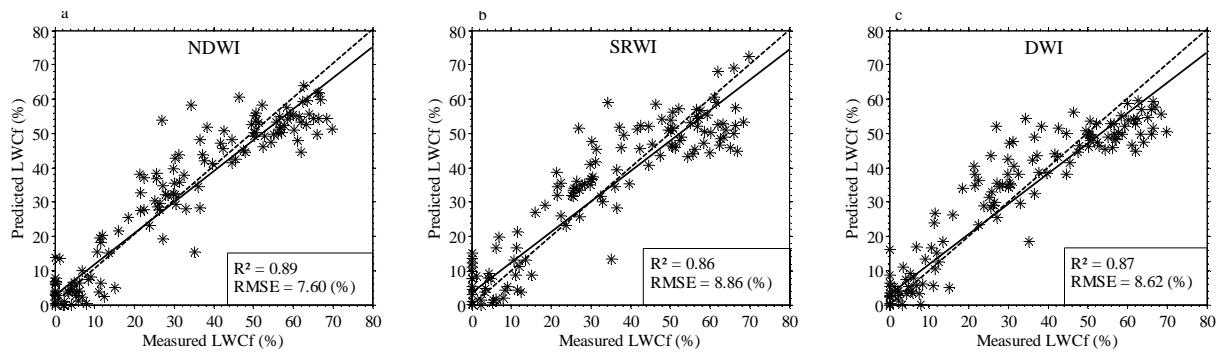
455



456

457 Figure 2. Contour map displaying the relationship (R^2) between leaf water content and different
 458 indices calculated from all possible waveband combinations from 0.390 – 2.50 μm . The blue
 459 rectangles represent the most sensitive waveband regions with the highest R^2 .

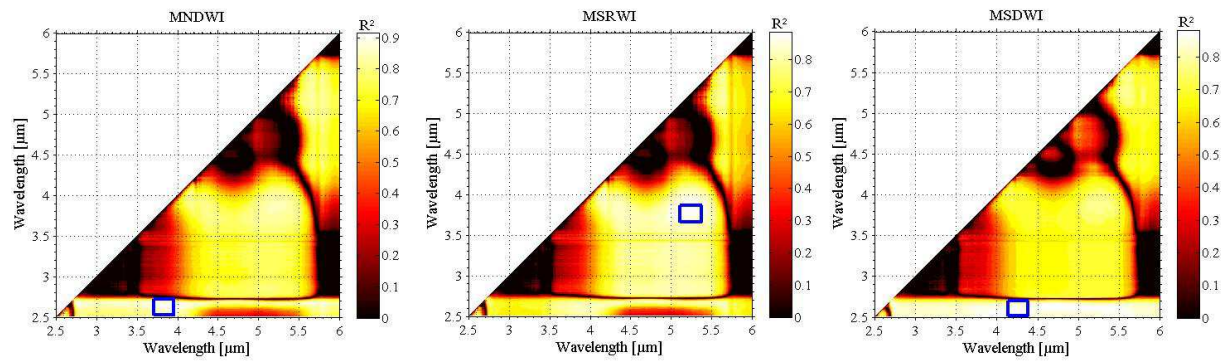
460



461

462 Figure 3. Scatterplots detailing the relationship between measured and predicted leaf water
 463 content using VNIR- SWIR. The solid line shows the regression line, while the dotted line is the
 464 1:1 line. The NDWI performed more accurately compared to SRWI and DWI.

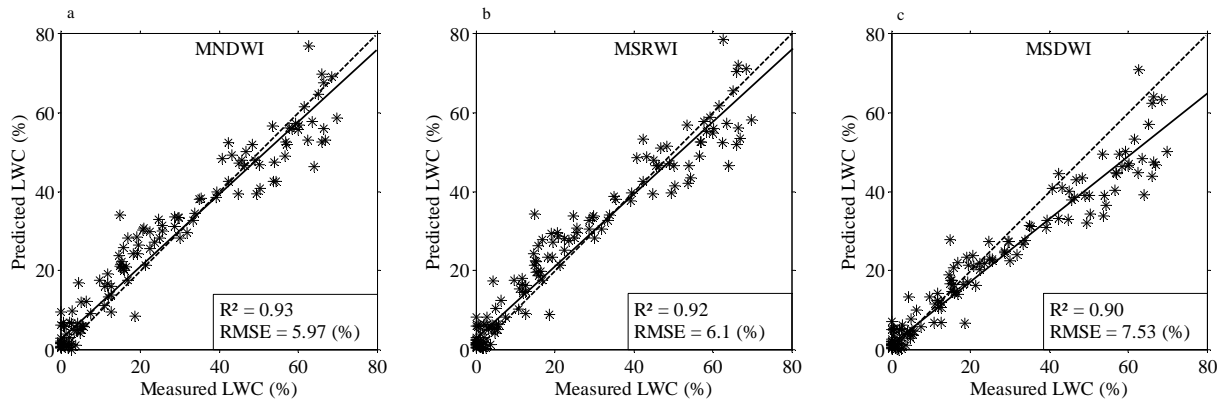
465



466

467 Figure 4. Contour map highlighting the relationship (R^2) between leaf water content and different
 468 indices calculated from all possible waveband combinations from 2.50– 6.00 μm . The sensitivity
 469 of different waveband combination is different. The blue rectangles represent the most sensitive
 470 waveband regions with the highest R^2 .

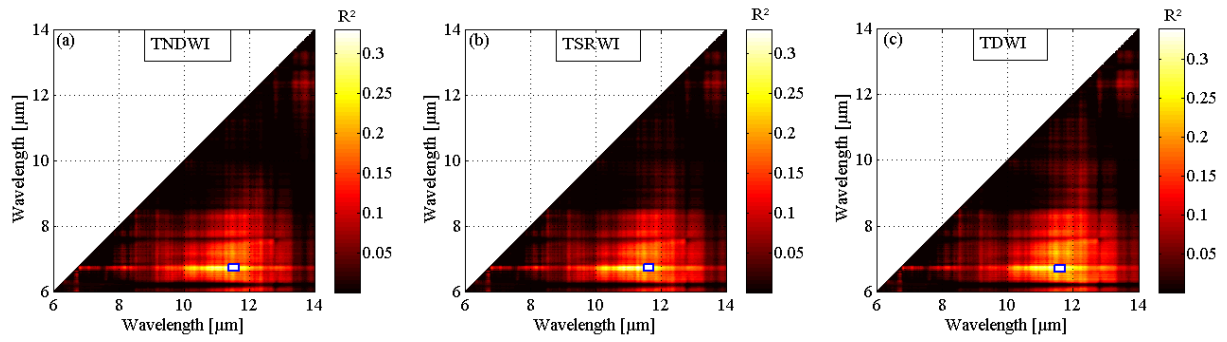
471



472

473 Figure 5. Scatterplot detailing the relation between measured and predicted leaf water content
 474 (LWC_f (%)). The predicted leaf water content is based on the calibration models developed from
 475 MNDWI, MSRWI and MSDWI; the highest correlation shown produced using MNDWI.

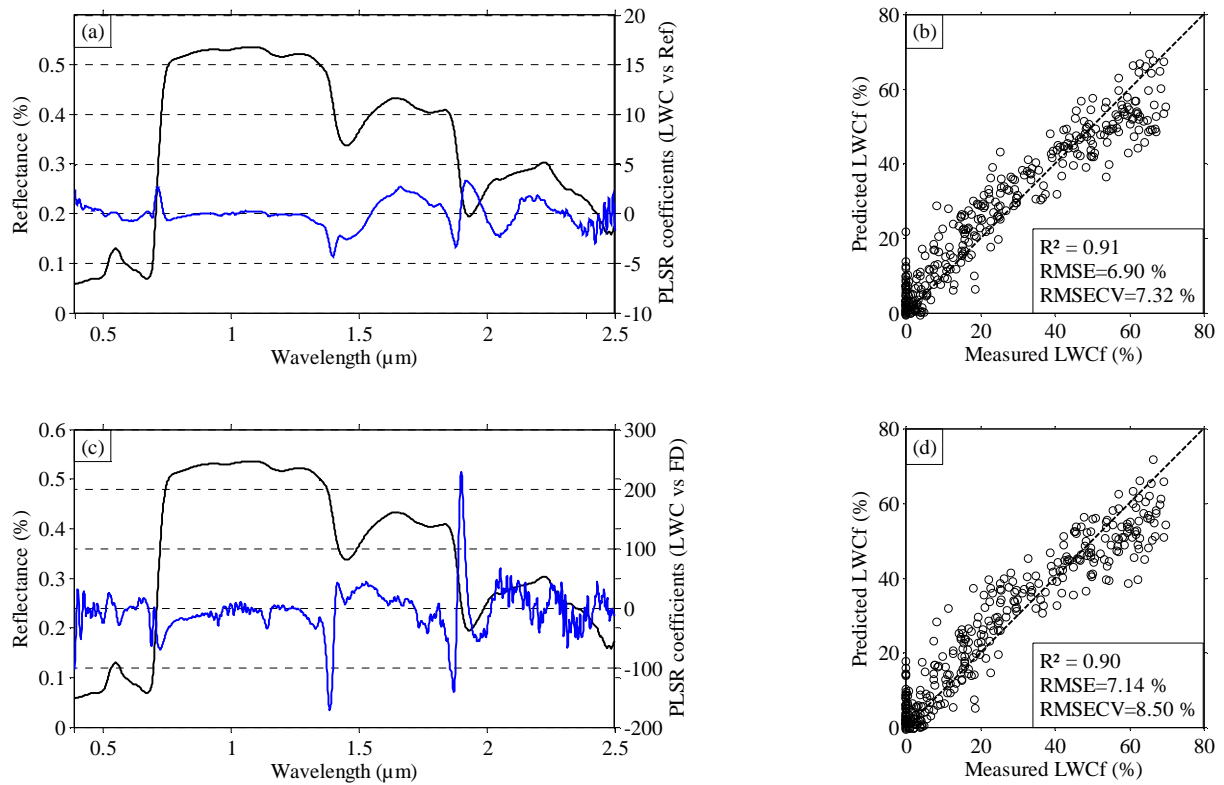
476



477

478 Figure 6. The relationships between leaf water content and narrow-band spectral indices in the
 479 TIR spectra. The rectangular region indicates the sensitive wavebands combination selected on
 480 the basis of the highest R^2 values.

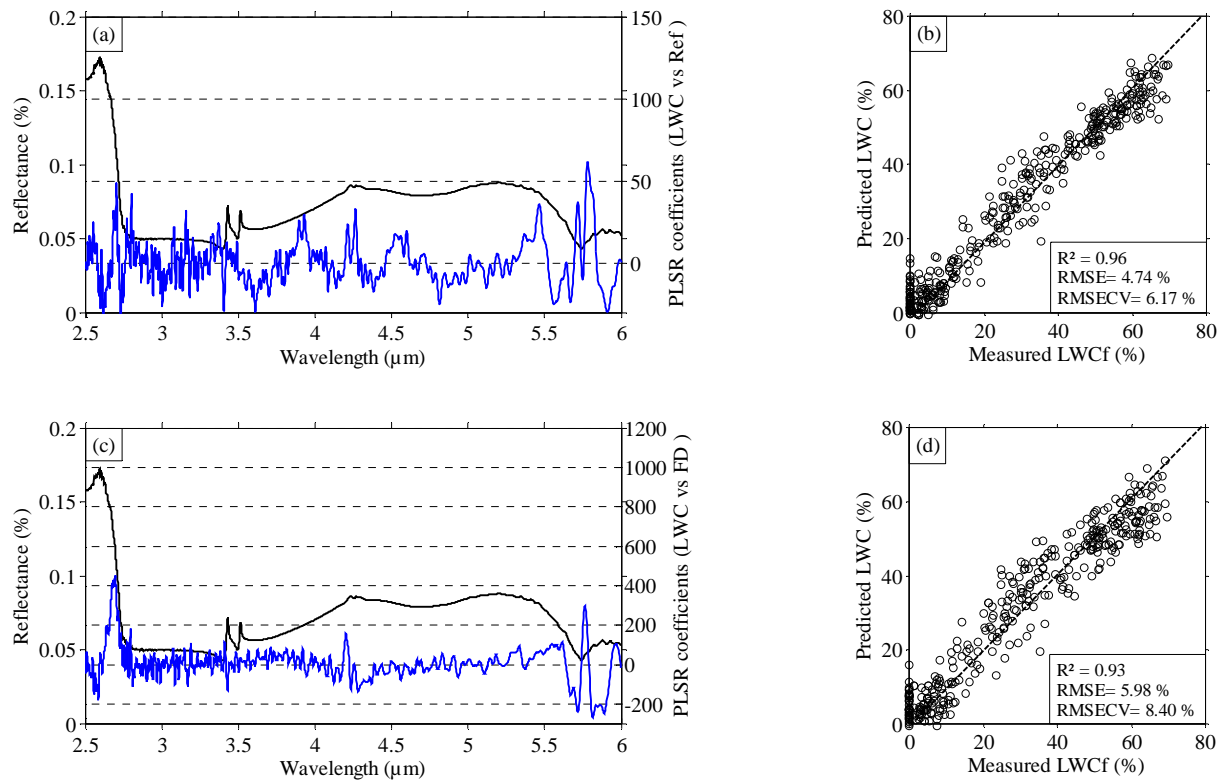
481



482

483 Figure 7. The PLSR coefficients (blue line) showing the importance of each waveband in
 484 developing the PLSR model for retrieving leaf water content from reflectance (a) and first
 485 derivative spectra (c) in the VNIR-SWIR. The average reflectance spectra (black line) are shown
 486 for reference purpose. The PLSR analysis using reflectance (b) predicted leaf water content more
 487 accurately (high R^2 and low RMSE and $RMSE_{cv}$) compared to the PLSR model developed from
 488 first derivative spectra (d).

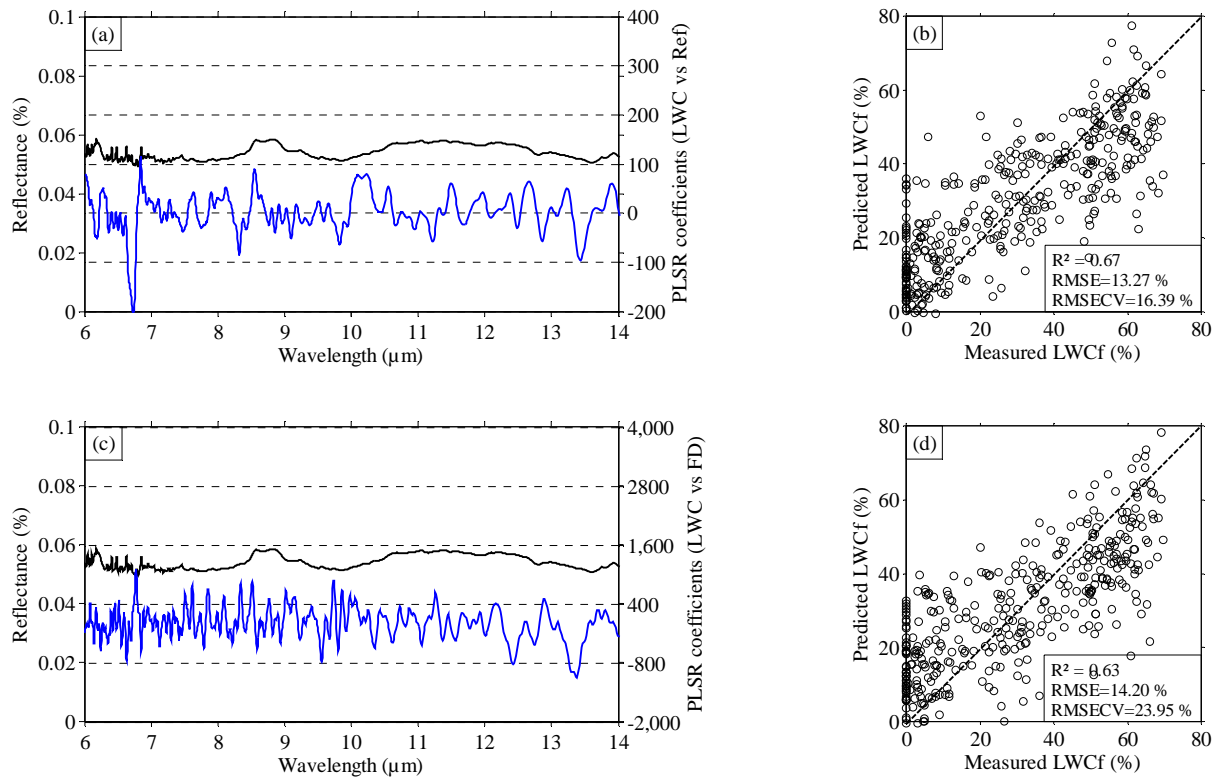
489



490

491 Figure 8. The PLSR coefficients (blue line) showing the importance of each waveband in
 492 developing the PLSR model for retrieving leaf water content from reflectance (a) and first
 493 derivative spectra (c) in the MIR. The average reflectance spectra (black line) are shown for
 494 reference purpose. The PLSR analysis using reflectance (b) predicted leaf water content more
 495 accurately (high R^2 and low RMSE and RMSE_{cv}) compared to the PLSR model developed from
 496 first derivative spectra (d).

497



498

499 Figure 9. The PLSR coefficients (blue line) showing the importance of each waveband in
 500 developing the PLSR model for retrieving leaf water content from TIR reflectance spectra (a).
 501 The average TIR reflectance spectra (black line) are shown for reference purpose. The PLSR
 502 models using TIR reflectance spectra (b) and TIR first derivative spectra (d) yielded moderately
 503 accurate estimate of leaf water content.

504

505 **List of Tables**

506 Table 1. Eleven plant species, their common name, Latin name, leaf sample size per species,
 507 successive drying phases, and the total number of spectra measured.

Common name	Species name	Sample size	Progressive drying phases	Total spectra
<i>Maidenhair tree</i>	<i>Ginkgo biloba</i>	6	6	36
<i>English ivy</i>	<i>Hedera helix</i>	6	8	48
<i>Norway Maple</i>	<i>Acer platanoides</i>	6	5	30
Redosier Dogwood	<i>Cornus sericea</i>	6	6	36
Japanese Knotweed	<i>Fallopia japonica</i>	6	5	30
Oriental Planetree	<i>Platanus orientalis</i>	6	6	36
Rhododendron	<i>Rhododendron caucasicum</i>	6	8	48
Largeleaf Linden	<i>Tilia platyphyllos</i>	6	6	36
Sweetgum	<i>Liquidambar styraciflua</i>	6	7	42
European Beech	<i>Fagus sylvatica</i>	6	4	24
Horse-Chestnut	<i>Aesculus hippocastanum</i>	6	6	36
	Calibration Dataset = 268		Validation dataset = 134	Total = 402

508

509

510

511 Table 2. List of spectral indices used in this study.

Name	Acronym			Equation
	VNIR-SWIR	MIR	TIR	
Normalized Difference Water Index	NDWI	MNDWI	TNDWI	$(R_{\lambda_1} - R_{\lambda_2}) / (R_{\lambda_1} + R_{\lambda_2})$
Simple Ratio Water Index	SRWI	MSRWI	TSRWI	$R_{\lambda_1} / R_{\lambda_2}$
Difference Water Index	DWI	MDWI	TDWI	$R_{\lambda_1} - R_{\lambda_2}$
where R_{λ_1} and R_{λ_2} is the reflectance at two different wavebands				

512

513

514 Table 3. The most sensitive wavebands for the different indices, selected on the basis of the
 515 highest R^2 values, and regression equations as calculated using the calibration datasets. The
 516 validation RMSE and R^2 are displayed in the last two columns.

Index	Most sensitive bands		Calibration		Validation	
	$\lambda_1(\mu\text{m})$	$\lambda_2(\mu\text{m})$	R^2	Regression Eq	R^2	RMSE (%)
NDWI	1.400	1.578	0.91	$y = -0.002x + 0.0368$	0.89	7.60
SRWI	1.397	1.614	0.88	$y = -0.0038x + 1.0694$	0.86	8.86
DWI	1.396	1.615	0.87	$y = -0.0014x + 0.0339$	0.87	8.62
MNDWI	2.651	3.891	0.92	$y = -0.0088x + 0.5562$	0.93	5.97
MSRWI	3.814	5.219	0.92	$y = 0.0092x + 0.5396$	0.92	6.10
MDWI	2.591	4.220	0.91	$y = -0.0024x + 0.1519$	0.90	7.53
TNDWI	6.730	11.310	0.34	$y = -0.0032x + 0.9632$	0.33	31.22
TSRWI	6.730	11.310	0.33	$y = -0.0019x - 0.0196$	0.32	31.83
TDWI	6.730	11.460	0.34	$y = -0.0002x - 0.0016$	0.32	31.69

517

518

519 Table 4. The results of PLSR analysis for estimating leaf water content using the reflectance and
 520 first derivative spectra in the VNIR-SWIR, MIR and TIR.

	Spectral region	No. of factors	R ²	RMSE (%)	RMSE _{CV} (%)
Reflectance spectra	VNIR-SWIR	8	0.91	6.90	7.32
	MIR	10	0.96	4.74	6.14
	TIR	9	0.67	13.27	16.39
First Derivative Spectra	VNIR-SWIR	8	0.90	7.14	8.50
	MIR	4	0.93	5.98	8.40
	TIR	4	0.63	14.21	23.95

521